

MODELLING OF GRANULAR FLOWS THROUGH INCLINED ROTATING CHUTES USING A DISCRETE PARTICLE MODEL

S.S.(Sushil) Shirsath,¹⁾ J.T.(Johan) Padding,¹⁾ H.J.H.(Herman) Clercx,^{2,3)} and J.A.M.(Hans) Kuipers¹⁾

¹⁾ Multiphase Reactors, Chemical Engineering and Chemistry, Eindhoven University of Technology, PO Box 513,
5600 MB, Eindhoven, The Netherlands

²⁾ Department of Physics and J.M. Burgers Center for Fluid Dynamics, Eindhoven University of Technology, P.O.
Box 513, 5600 MB Eindhoven, The Netherlands

³⁾ Department of Applied Mathematics, University of Twente, P.O. Box 217, 7500 AE Enschede, The Netherlands

ABSTRACT

In blast furnaces, particles like coke, sinter and pellets enter from a hopper and are distributed on the burden surface by a rotating chute. Such particulate flows suffer occasionally from chocking and particle segregation at bottlenecks, which hinders efficient throughflow. To get a more fundamental insight into these effects, we started a combined experimental and numerical program to investigate such particulate flows. For this purpose we employ discrete particle model simulations of granular monodisperse and bidisperse particles flowing down inclined rotating chutes. In these simulations, non-inertial effects due to rotation are implemented through Coriolis and centrifugal forces. A rolling resistance model is also implemented to study the effect of a non-spherical shape of the particle. In addition, a granular chute flow set-up has been constructed for experimental validation of the model. Different measurement techniques will be used to measure the solid fraction, particle velocity, granular temperature and bed height in the chute, which are compared with the results from discrete particle model simulations. The influence of polydispersity, non-uniformity of particles, rotation speed and angle of inclination of the chute will be studied.

Here we present results obtained from preliminary simulations for the averaged particle velocity, bed height and granular temperature along the length of chute for different rotation speeds. We find an interesting interplay between the Coriolis force, which pushes the granular flow to the sidewall of the chute and decelerate the flow, and centrifugal forces that accelerate the flow.

Keywords: Granular flow, discrete particle model, rolling resistance model, rotating chute;

NOMENCLATURE

g	Gravitational acceleration (m/s^2)
ϕ	Inclination angle of system (deg)
Ω	Angular velocity of system (rad/s)
m	Mass of particle (kg)

r	Position of particle (m)
V	Velocity of particle (m/s)
F	Force on particle (N)
I	Moment of inertia of particle ($kg\ m^2$)
ω	Angular velocity of particle (rad/s)
T	Torque on particle (N m)
μ	Coefficient of static friction (-)
μ_r	Coefficient of rolling friction (-)
e	Coefficient of restitution (-)
k	Normal spring stiffness (N/m)
d	Particle diameter (m)
ρ	Particle density (kg/m^3)
N	Number of particles (-)
θ	Granular temperature (m^2/s^2)

Subscripts

p	particle
r	rolling
k	cell
n	normal
t	tangential

INTRODUCTION

The flow of granular matter in a rotating system is an important phenomenon in many industrial fields. In rotating systems such as rotating inclined chutes, the flow behavior of granular material is greatly affected by the Coriolis and centrifugal forces. As a consequence, the flow path in a rotating chute deviates considerably from that in a non-rotating chute. This results in a concentration gradient across the cross-section of a rotating chute. The study of (rotating) granular flows is also of fundamental interest, with many challenges from both an experimental and numerical point of view.

An important application of granular flow is in the blast furnace in the steel industry for distribution of material

through a rotating chute. A blast furnace is a reactor for reducing the iron ore to pig-iron, as has been traditionally used in the world. The iron ore and the coke particles are deposited in the blast furnace in alternating layers, and the gas is blown from the tuyeres at high temperature. A great effort has been spent on improving the productivity. Mixing of nut coke particles with the iron ore is particularly employed to enhance the efficiency of reductive reaction of iron ore, because it increases the contact frequency between the iron ore and the coke particles (Shimomura et al. (1976), Okuda et al.(1983), Isobe et al. (1990), Watanabe et al. (2006), Babich et al. (2009)). The size of the nut coke particles is generally the same as that of iron ore. However the density of coke is much smaller. Thus, it is important to understand particle segregation caused by the density difference taking place during delivery to the blast furnace. There are a lot of storages, bunkers, conveyors and chutes on the way to the blast furnace, and the particles are usually segregated during the repetitive charging and discharging processes. The goal is to prevent or undo such particle segregation.

Computational simulation using a Discrete Particle Model (DPM) is one of the most useful tools for the analysis, visualization, and study of closure relations for the granular flow behavior during transport (Weinhart et al. (2012), Thornton et al. (2012)). In DPM the solid elements are tracked individually. The strong point of this method is that, once validated by direct comparison with the experiments, it allows for calculating physical quantities that are difficult or impossible to measure in experiments.

In particular, industrial processing in the steel industry concerns the controlled charging of blast furnaces with coke, sinter and pellets through open rotating chutes. Despite their common occurrences, fundamental knowledge about the dynamics of these particulate flows through (rotating) chutes is lacking. The particulate flows suffer occasionally from chocking and particle segregation at bottlenecks, providing challenges for efficient through-flow. This seriously jeopardizes continuous operation of the production line and can lead to costly down-time. The influence of both chute rotation and the irregular shape of the particles on the dynamics and segregation of particulate flows are poorly understood, yet understanding is required to control the particle inflow rate and chute rotation rate such that costly bottlenecks in the production process can be avoided.

A version of the Discrete Particle Model - usually used for gas-solid fluidized beds (Hoomans et al. (1996), Van der Hoef et al.(2006)) - is modified to allow for simulation of particle flows through a chute rotating around an axis parallel to gravity. The geometry of the simulated channel, the rotation axis, and its orientation with respect to gravity are represented in Fig. 1.

In the present paper we investigate the effect of rotation, of a smooth-wall chute fixed at an angle of inclination of 30 degrees, on the flow of dry granular material. We investigate two cases: (1) monodisperse particles, and (2) a binary mixture of same sized particles of small and large density. We will show that chute rotation has a pronounced effect on the distributions of particle positions, average velocities, velocity fluctuations, and density segregation.

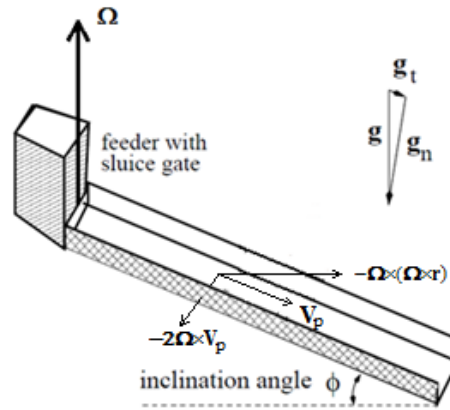


Figure 1: Chute geometry. Here, \mathbf{g} is the gravitational acceleration and Ω is the angular velocity of the chute rotating around an axis going through the feeder sluice gate. The velocity \mathbf{V}_p of a particle located at \mathbf{r} relative to the rotation axis will be directed mainly along the length of the chute. In a co-rotating frame of reference, the particle feels a Coriolis acceleration sideways and a centrifugal acceleration away from the rotation axis.

MODEL

Equations of motion

The translation and rotation of every individual particle P in the system is described by Newton's equations:

$$m_p \frac{d\mathbf{V}_p}{dt} = m_p \mathbf{g} + \mathbf{F}_{contact} \quad (1)$$

$$I_p \frac{d\boldsymbol{\omega}_p}{dt} = \mathbf{T} \quad (2)$$

Here m_p is the mass of particle P , and I_p the moment of inertia around its center-of-mass. The forces on the right hand side of eq. (1) are, respectively, due to gravity and contact forces. The contact forces are caused by collisions with other particles or confining walls. The torque \mathbf{T} on a particle is also determined by these contact forces. For completeness, we note that in preliminary simulations we have also studied the effect of pressure and drag forces induced by the co-flowing interstitial gas. Because we found no significant change in the results, we ignore gas-induced forces in the rest of our analysis.

Contact model

Soft sphere model

The particle-particle contact force model accounts for energy dissipation by means of empirical coefficients of normal and tangential restitution, the coefficient of friction, and a rolling friction. Apart from the rolling friction, we employ a standard linear spring/dashpot model, wherein

separate springs and dashpots are defined for normal and transversal displacements. The velocities, positions and contact forces of the particles are calculated at every fixed time step via a first order time integration. A schematic representation of the linear spring/dashpot soft-sphere model is shown in figure 2. For more details on the implementation of the soft-sphere model we refer to the work of Van der Hoef et al. (2006) and Deen et al. (2006).

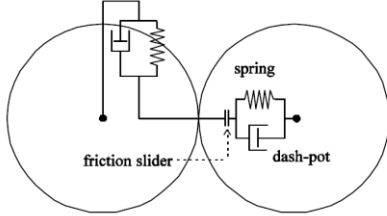


Figure 2: Schematic representation of the linear spring/dashpot soft-sphere model.

Rolling resistance model

We include a rolling friction in our DPM simulations to account for the fact that real particles are never perfectly spherical. Actually, particles in industrial processes such as in the steel industry are of a completely irregular shape. The most accurate solution would be to model the exact particle shape. However, this is computationally very expensive because of the large increase in the number of degrees of freedom and more expensive statistical ensemble averaging. Simulating the exact shape is therefore not suitable to simulate granular flow in industrial processes. The particle shape mainly affects the particle rotation velocity and particle packing fraction. As a first approximation we will still treat the particles as spherical, but with an additional rolling friction to account for the decrease in rotation velocity, as described by Zhou et al. (1999). In detail, besides the usual soft-sphere friction torque, we introduce an additional rolling resistance torque on a particle A due to interactions with a particle B, as follows:

$$\mathbf{T}_r = -\mu_r R_r F_n \frac{\boldsymbol{\omega}_{rel}}{|\boldsymbol{\omega}_{rel}|} \quad (3)$$

$$\boldsymbol{\omega}_{rel} = \boldsymbol{\omega}_A - \boldsymbol{\omega}_B \quad (4)$$

Here $\boldsymbol{\omega}_A$ and $\boldsymbol{\omega}_B$ are the angular velocities of particle A and B respectively, $\boldsymbol{\omega}_{rel}$ is the relative angular velocity between them, and $|\boldsymbol{\omega}_{rel}|$ its magnitude. The rolling resistance torque is assumed to scale linearly with the magnitude of the normal force F_n between particles A and B and with the rolling radius R_r is given by

$$R_r = \frac{r_A r_B}{(r_A + r_B)} \quad (5)$$

Here r_A and r_B are the radii of the two particles. The dimensionless coefficient of static friction μ from the soft-

sphere model and the coefficient of rolling friction μ_r from the above model together determine the rolling behaviour of the particles. For a perfectly smooth sphere $\mu_r=0$, and the static friction at the surface of the sphere causes a rolling motion without sliding. For a very irregularly shaped particle (imagine a square block) $\mu_r > \mu$, and the particle always slides without rolling. For nearly-spherical particles we have $0 < \mu_r < \mu$, and particles can both slide and roll. In our work we assumed the latter.

Coriolis and centrifugal forces

Although it is possible to let a chute rotate in our computational domain, it is computationally more efficient to work in a frame of reference co-rotating with the chute. In such a case apparent forces arise due to the non-inertial motion of the system. Every particle P in the rotating system experiences an additional Coriolis and centrifugal force, which are added to the above equation of motion (1):

$$(\mathbf{F})_{rotating} = (\mathbf{F})_{stationary} - 2m_p(\boldsymbol{\Omega} \times \mathbf{V}_p) - m_p(\boldsymbol{\Omega} \times [\boldsymbol{\Omega} \times \mathbf{r}]) \quad (6)$$

Here $\boldsymbol{\Omega}$ is the angular velocity of the chute and \mathbf{r} the position of the particle relative to the axis of rotation through the feeder sluice gate. The rotation axis and the directions of the Coriolis and centrifugal accelerations are indicated in Figure 1.

Similarly, every particle will experience an additional Coriolis torque, which must be added to equation (2):

$$(\mathbf{T})_{rotating} = (\mathbf{T})_{stationary} - I_p(\boldsymbol{\Omega} \times \boldsymbol{\omega}_p) \quad (7)$$

Inclusion of a Coriolis torque is necessary because, even when no explicit torques apply to a particle, in the co-moving frame of reference the direction of the particle angular momentum will reorient. This reorientation is such that when viewed from an outside inertial system, the angular momentum is actually conserved.

Simulation parameter settings

We have chosen our simulation parameters to match the properties of an experimental lab-scale set-up. The experimental set-up consists of a chute of 90 cm length and 8 cm width, through which we flow particles with a diameter of 3 mm. The particle material is either glass (the high density material) or plastic (the low density material). Simulations are performed for rotation rates of 0, 2, 4, 8 and 16 rotations per minute (rpm). We choose this particular range because we expect a transition in behavior to occur within this range. An important dimensionless number for this transition is the Rossby number, defined as

$$Ro = \frac{U}{\Omega L} \quad (8)$$

where U is a typical velocity (within the co-rotating frame) and L is a typical distance to the rotation axis. When the

Rosby number becomes less than order unity, a transition in the system behavior is expected. In our system typical particle velocities are of the order of 1 m/s and the typical distance of the order of 1 m; we therefore expect transitions to occur at a rotation rate of the order of 1 rad/s or 10 rpm. We note that the dimensions of our experimental setup are smaller than the charging system used in actual industrial practice. However, to accurately assess the *relative* effect of rotation on the granular flow it is more important to match the Rosby number of the industrial setup which is close to 1.5. This is included in the range of Rosby numbers studied in our experiments and simulations. The system properties and operating conditions are specified in Table 1.

Property	Value	unit
Chute width	0.08	m
Chute depth	0.045	m
Chute length	0.9	m
Chute inclination angle	30	degrees
Number of particles (typical)	40000	-
Particle diameter	0.003	m
Particle density 1	2470	kg/m ³
Particle density 2	900	kg/m ³
Normal spring stiffness	100	N/m
Coefficient of normal restitution	0.97	-
Coefficient of tangential restitution	1.0	-
Coefficient of static friction	0.344	-
Coefficient of rolling friction	0.05	-
Total simulation time	6	s
Time step	2.5e-05	s

Table 1: Simulation setting for granular chute flow

The simulation parameters for glass beads are obtained from Vreman et al. (2007). We are in the progress of obtaining all single particle collision and rolling parameters from independent experimental measurements. However, to focus on the density difference effect, in the simulations reported in this work we use the same coefficients of restitution and the same friction coefficients for the plastic beads as for the glass beads. Moreover, to enable a fair comparison between the simulations and the experiments, a constant mass flow rate of 1.6 kg/s was applied at the inlet.

SIMULATION RESULTS

In this section, we discuss the flow behaviour of monodisperse and bidisperse (in density) dry granular materials down a rotating inclined chute. We study the effects of different rotation rates on the particle velocity, granular temperature and the height of the particle bed.

Monodisperse granular flow through an inclined rotating chute

Snapshots of monodisperse flow simulations are shown in Figure 3, where we colored the particles according to their velocities. For the non-rotating chute (0 rpm) there is an accelerating downward flow of particles. At elevated rotation rates the velocities increase even more (due to centrifugal forces) and the particles move to the right with respect to the flow direction (due to the Coriolis force). Once a steady state is reached in the chute, time averages of the particle velocity, bed height and granular temperature (velocity fluctuations) are calculated.

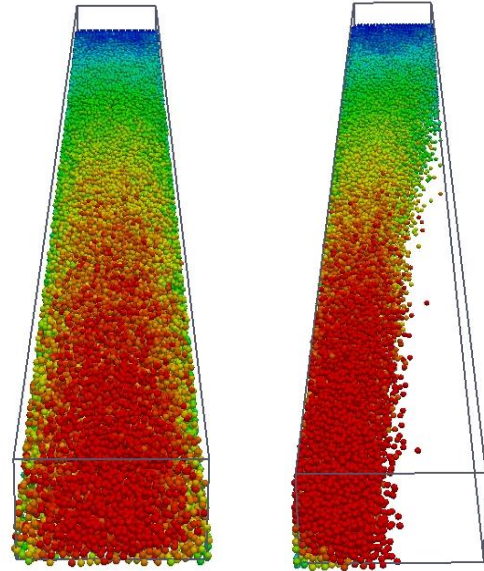


Figure 3: Snapshots of particle velocity of dry monodisperse granular flow in the chute for rotation rates of 0 and 16 rpm.

Particle velocity

Figure 4 shows the cross-sectional averaged particle velocity in the (z) direction along the length of the chute for different rotation rates. As the rotation rate increases, there is a slight decrease in average velocity in the first half of the chute. This may be understood to be a consequence of the Coriolis force which drives the particles towards the sidewall, leading to compaction and an increased friction with the sidewall. In the second half of the chute the picture is reversed, and the average z-velocity increases with increasing rotation rate. Here, the centrifugal force plays an important role, increasingly accelerating the particles with increasing distance from the chute rotation axis.

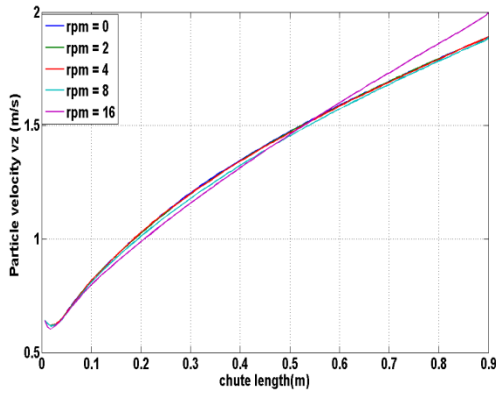


Figure 4: Time averaged particle velocity along the length of the chute for different rotation rates (see legend) and a fixed angle of inclination of 30 deg.

Bed height

Figure 5 shows the height of the particle bed in the chute along the length of the chute for different rotation rates. We have estimated this height as twice the height of the center-of-mass of all particles at a certain z-position. The average height is maximum at the inlet of the chute, quickly decreases in the first 10 cm of the chute, and then slowly decreases along the remainder of the length of the chute.

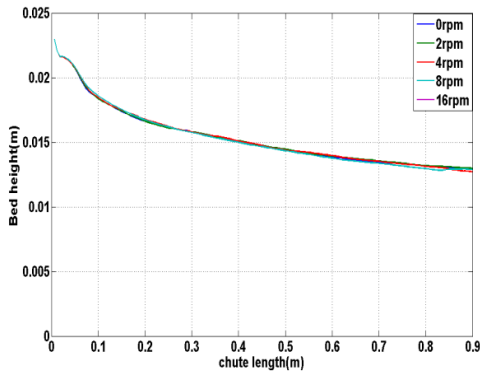


Figure 5: Time averaged particle bed height for different rotation rates and a fixed angle of inclination of 30 deg, as estimated from the center-of-mass height at different locations along the length of the chute.

Figure 5 suggests that, as the rotation rate of the chute increases, the average height of the particle bed along the length of the chute hardly changes. This is rather deceptive because under rotation the particle bed height is not uniform in the cross-section of the chute, as shown in Figure 6. The maximum particle bed height in the chute actually increases locally with increasing rotation rate as a consequence of the Coriolis force pushing the particles against the sidewall.

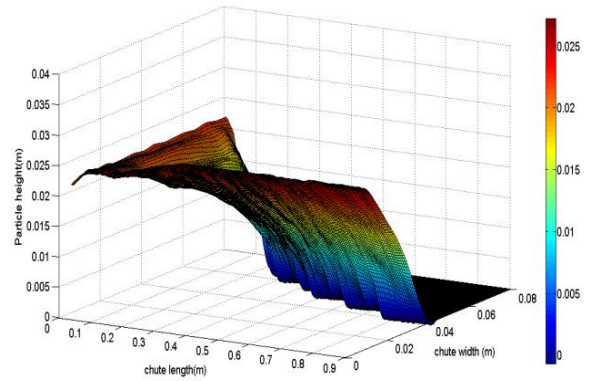


Figure 6: Surface plot for the average particle bed height for a rotation rate of 16 rpm and an angle of inclination of 30 deg of the chute.

Granular temperature

The DPM simulation data allow us to calculate the granular temperature, which is a measure for the particle velocity fluctuations due to particle-particle interaction. The granular temperature is a very important quantity in the kinetic theory of granular flow (KTGF) (e.g. Gidaspow, 1994; Balzer et al., 1995; Nieuwland et al., 1996). DPM simulations can be used to verify the basic assumptions underlying the KTGF. In this work we use the DPM to gain insight in the effect of chute rotation on the granular temperature. The granular temperature at a particular time in a cell k is computed as,

$$\theta_k = \frac{1}{3} \frac{\sum_i^{N_{part,k}} (\mathbf{v}_i - \langle \mathbf{v}_p \rangle_k)^2}{N_{part,k}} \quad (9)$$

Here, \mathbf{v}_i is the velocity of a particle i in cell k and $\langle \mathbf{v}_p \rangle_k$ is the average particle velocity in that cell at a particular time. The sum runs over all $N_{part,k}$ particles inside the cell at that particular time.

Figure 7 shows the time averaged granular temperature along the length of the chute for different rotation rates of the chute. In all cases we observe a gradual increase in granular temperature as the particles flow down the chute. At low rotation rates up to 4 rpm the dependence is almost the same as for the non-rotating case. At higher rotation rates we observe a similar behaviour as for the average velocity: in the first half of the chute the granular temperature is lowered because of compaction forces (Coriolis force), whereas in the second half of the chute the granular temperature is increased because of the increasing effect of the centrifugal force.

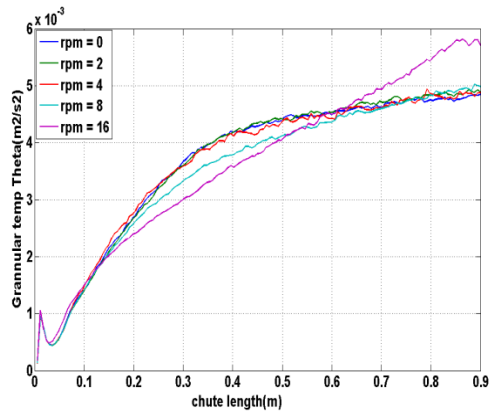


Figure 7: Time averaged granular temperature along the length of the chute for different rotation rates of the chute and a fixed angle of inclination of 30 deg.

Bidisperse granular flow through an inclined rotating chute

In the next set of simulations, we simulated the flow of a binary mixture of two different density particles through a rotating inclined chute. We used a uniform size of particles equal to a diameter of 3 mm, and a density of 2470 kg/m³ and 900 kg/m³, respectively. The two different types of particles are introduced at the inlet of the chute in a randomly mixed fashion with a particle number ratio of 1:1 and a constant mass flow rate of 1.6 kg/s. Snapshots of a non-rotating (0 rpm) and rotating system at 16 rpm are shown in Figure 8.

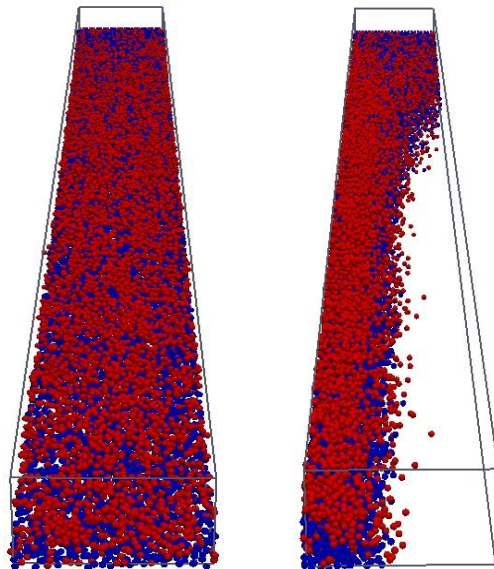


Figure 8: Snapshots of a simulation of a binary mixture flowing through an inclined chute at a fixed angle of 30 deg without (left) and with (right) rotation at 16 rpm. Color coding is for the particle density. Blue: 2470 kg/m³ and Red: 900 kg/m³

For the simulation of the granular flow in the rotating chute the setting of parameters and the boundary conditions used are the same as those summarized in Table 1.

Particle velocity

Figure 9 shows the particle velocity of large and small density, respectively, along the length of the chute for different rotation rates. After a certain length, the small density particles clearly move faster than the large density particles. This is a first indication that the initial random mixture segregates into a small density top layer and high density bottom layer: because the top layer is not in direct contact with the bottom wall, it experiences a smaller friction than the bottom layer, and consequently moves faster.

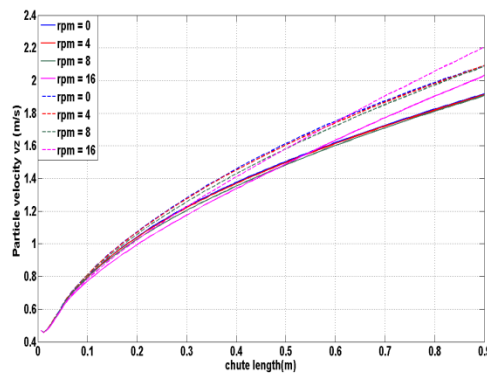


Figure 9: Time averaged particle velocities for two different densities particles along the length of the chute for different rotation rates (see legend) and a fixed angle of inclination of 30 deg. Solid lines are for the high density (2470 kg/m³) and dashed lines for the low density (900 kg/m³) particles.

Center of mass height

Figure 10 shows the center-of-mass height perpendicular above the bottom wall of the chute for the high and low density particles as a function of location along the length of the chute, for different rotation rates and at fixed angle of 30 deg. Because a random mixture is introduced at the inlet of chute, the center of mass for both particles is initially the same. As the particles flow downwards along the chute, they segregate into a low density top layer and high density bottom layer. Again it should be noted that the center-of-mass height is not uniform across the cross-section of the chute which becomes apparent from two-dimensional plots (not shown here).

Granular temperature

Figure 11 shows the time averaged granular temperature for low and high density particles along the length of the chute for different rotation rates of the chute and for fixed angle of inclination of 30 deg. The granular temperature for both type of particles is minimum near the inlet due to very low velocity fluctuation between the particles and it increases in

the flow direction. The velocity fluctuations are higher for the low density particles than for the high density particles, in a ratio that is roughly given by equipartition of the kinetic energy. At small rotation rates, we observe the same behavior as in a nonrotating chute. As the rotation rate increases the granular temperature slightly decreases in the first half of the chute (again due to compaction forces) and clearly increases in the second half, presumably by the centrifugal forces. We will focus on these aspects in greater detail in a forthcoming paper.

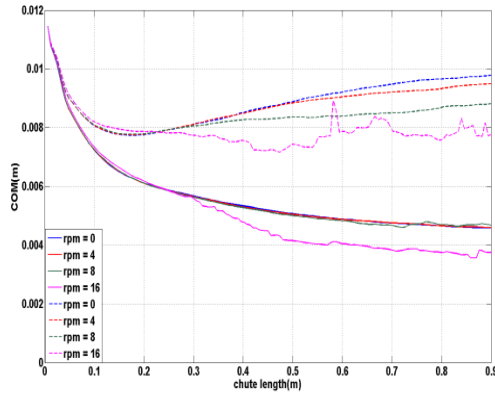


Figure 10: Time averaged Center of mass for two different densities particles along the length of the chute for different rotation rates (see legend) and a fixed angle of inclination of 30 deg. Solid lines are for the high density (2470 kg/m^3) and dashed lines for the low density (900 kg/m^3) particles.

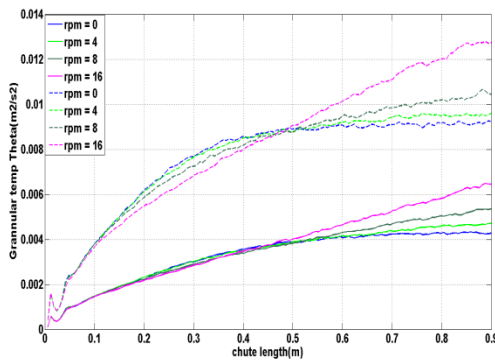


Figure 11: Time averaged granular temperature for two different densities particles along the length of the chute for different rotation rates (see legend) and a fixed angle of inclination of 30 deg. Solid lines are for the high density (2470 kg/m^3) and dashed lines for the low density (900 kg/m^3) particles.

CONCLUSIONS

In this paper we presented DPM simulation results of dry granular flows down a rotating chute inclined at fixed angle of inclination of 30 deg. The observed flow patterns mainly depend on the rotation rate of the chute. In all cases, with

increasing rotation rate the particles are moving increasingly to the right sidewall with respect to the mean flow in the chute. The particle velocity and granular temperature are slightly reduced in the first half length of the chute due to compaction as result of the Coriolis force but strongly increase in the second half due to the increasing importance of the centrifugal forces. For the monodisperse simulations, the particle bed height becomes a two-dimensional function of the position inside the chute, with a strong increase in bed height along the sidewall due to the Coriolis forces. For the bidisperse simulations, the segregation of small and large density particles is most pronounced in the second half of the chute and becomes stronger with increasing rotation rate.

ACKNOWLEDGEMENT

The authors acknowledge STW (project: 11039) for their financial support and Tata Steel BV (IJmuiden), Unilever B.V. Netherlands and BASF Ludwigshafen, Germany for their technical support. We thank M.A. van der Hoef for his initial guidance for this project. Special thanks go to O. Bokhove, A.R. Thornton and D. Tunuguntla for their input into this project.

REFERENCES

- SHIMOMURA, Y. KUSHIMA, Y. SATO, F. AND ARINO, S.,: TETSU-TO-HAGANÉ, 62 (1976), S404.
- OKUDA, K. AMANO, S. ISHIOKA, N. ONO, H. FURUKAWA, T. AND INOUE, T.,: TETSU-TO-HAGANÉ, 69 (1983), S731.
- ISOBE, M. SUGIYAMA, T. AND INABA, S.,: *Proc. 6th Int. Iron Steel Cong.*, ISIJ, Tokyo, 2 (1990), 439.
- WATANABE, S. TAKEDA, K. NISHIMURA, H. GOTO, S. NISHIMURA, N. UCHIDA, T. AND KIGUCHI, M.,: TETSU-TO-HAGANÉ, 92 (2006), 901.
- BABICH, A. SENK, D. AND GUDENAU, H.W.,: *Ironmaking Steelmaking*, 36 (2009), 222.
- WEINHART, T. THORNTON, A.R. LUDING, S. AND BOKHOVE, O., "Closure relations for shallow granular flows from particle simulations", *Granular Matter* 14 (2012), 531.
- THORNTON, A. WEINHART, T. LUDING, S. AND BOKHOVE, O., "Modeling of particle size segregation: calibration using the discrete particle method", *Int. J. Modern Phys. C* 23 (2012), 1240014.
- HOOmans, P.B.P. KUIPERS, J.A.M. BRIELS, W.J. AND SWAAIJ, W.P.M. VAN., "Discrete particle simulation of bubble and slug formation in a two dimensional gas-fluidised bed: A hard-sphere approach", *Chem. Eng. Sci.*, 51(1996), 99-118.
- VAN DER HOEF, M.A. YE, M. VAN SINT ANNALAND, M. ANDREWS IV, A.T. SUNDARESAN,

S. & KUIPERS, J.A.M., Multi-scale modeling of gas-fluidized beds. *Adv. Chem. Eng.* **31**, (2006), 65.

VREMAN A.W. TARAZI M. AL. KUIPERS J.A.M.VAN SINT ANNALAND M. AND BOKHOVE, O., 2007. Supercritical shallow granular flow through a contraction: experiment, theory and simulation. *J. Fluid Mechanics*, Vol 578, 233-269.

ZHOU, Y.C. WRIGHT, B.D. YANG, R.Y. XU, B.H. and YU, A.B., Rolling friction in the dynamic simulation of sandpile formation, *Physica A* 269 (1999) 536–553.

DEEN, N.G. ANNALAND, M.V.S. and KUIPERS, J.A.M., Detailed computational and experimental fluid dynamics of fluidized beds. *Applied Mathematical Modelling*, 30(2006), 1459-1471.

GIDASPOW D., Multiphase flow and fluidization: Continuum and kinetic theory descriptions, (1994), *Academic press*, Boston

BALZER G. BOELLE A. SIMONIN O. Eulerian gas-solid flow modelling of dense fluidized bed, in 'Fluidization VIII' edited by J.-F. Large and C. Lagueré ie, *Engineering Foundation*, (1995) New York, 409-418

NIEUWLAND J.J. VAN SINT ANNALAND M., KUIPERS J.A.M., VAN SWAAIJ W.P.M., Hydrodynamic modeling of gas/particle flows in riser reactors, *AIChE J.*, 42, (1996) 1569-1582